Nigerian Research Journal of Engineering and Environmental Sciences 5(2) 2020 pp. 679-693

Nigerian Research Journal of Engineering and Environmental Sciences
Journal homepage: www.rjees.com

Original Research Article

Particle Overlay Obstruction Modelling, Parametric and Output Characteristics Evaluation of a Photovoltaic System

Ibeagwu, O.I., *Eke, M.N., Maduabuchi, C.C., Mgbemene, C.A. and Aka, T.V.

Department of Mechanical Engineering University of Nigeria, Nsukka, Enugu State, Nigeria.
*mkpamdi.eke@unn.edu.ng

ARTICLE INFORMATION

Article history:
Received 04 Aug, 2020
Revised 12 Oct, 2020
Accepted 14 Oct, 2020
Available online 30 Dec, 2020

Keywords:
Obstruction transmission models
Particle overlay
PV system
Soiling
Power output

ABSTRACT

This study theoretically investigated the obstruction models for overlaid dust particles on the surface of a Photovoltaic (PV) system. The models applied were the soiling overlay transmission models which was developed by NASA and Martin's model. These models were capable of incorporating the various dust sizes and predict the effect of dust obstruction on the output characteristics and other necessary parameters of PV systems. Simulation was done using MATLAB software. The results were calculated and compared with existing experimental results. The investigated models facilitated the prediction of PV performance under dusty conditions for different particle sizes irrespective of the location. From the study, the dusty system has less transmissivity and more heat loss than the dust free system. The power output and efficiency of the PV system was found to have percentage losses of 20.9% and 9.1% respectively for a mass density of 7.91 kgm^{-2}. The obstructed radiation influenced the current- voltage (I-V) characteristic under a dusty condition and it was observed that the adverse effect is also dependent on the type of dust. In comparison with experimental result in Karnataka, India, the maximum percentage deviation from the experimental result was 6.3% and 9% for the power loss and the current-voltage (I-V) characteristics.

© 2020 RJEES. All rights reserved.

1. INTRODUCTION

Photovoltaic panels are the most widely used solid state solar energy converters amidst all solar power systems. To date, owing to their low performance stemming mainly from increased module temperature, these modules have undergone steady and incremental development (Al-Waeli et al., 2017). Solar irradiance, solar panel inclination angle and dust depositions have shown a severe adverse effect on transmittance and performance of PV systems (Abdullah et al., 2014). These effects are observed to increase as the system keeps running (Bouchalkha 2008; Syed and Husam, 2014). In recent times, the focus of most

researchers is on the influence of dust deposition on the efficiency and power output of the system when the PV module are exposed to both natural and artificially influenced environment (Kaldellis et al., 2011; Hashim 2013; Sarver et al., 2013; Samadhiya and Pandey 2016; Paudyal et al., 2017). However, results obtained through experiments, though having similar conclusions would be difficult to model with a single mathematical relationship. This is because of variations in environmental conditions for different regions. There are very few researchers who have carried out studies on the physical features of particle deposition such as moisture content, particle size, chemical compositions, densities, soil index etc. (Zorrilla-Casanova et al., 2011; Mekhilefa et al., 2012; Ahmed et al., 2013; Appels et al., 2013; Sayyah et al., 2014; Dadas et al., 2016; Menoufi, 2017). However, few researches based on theoretical modelling have been carried out on the effect of dust deposition on photovoltaic panel transmittance which is an essential parameter. From the knowledge of the authors, hardly is there a literature that has modelled the overlay effect of a dusty PV system theoretically through thermodynamic analysis to incorporate particles of different sizes.

This paper thus presents a theoretical approach to study the overlay obstruction of dust deposition on PV panels. This is with a view to predict the operations of PV module under dusty condition for different particle sizes irrespective of the location or region.

2. METHODOLOGY

2.1. Theoretical Basis

To evaluate transfer and loss of energy, simple theoretical assumptions and mathematical models were used. In order to obtain the effect of dust on the incident angle of solar radiation, output characteristics of PV modules, transmissivity, efficiency and other performance losses, model equations such as thermodynamic energy model, proven overlay dust models and electrical analysis models were applied. The models applied were overlay models developed by the National Aeronautics and Space Administration (NASA) to describe the influence of dust deposition on solar PV modules (Katzan and Edwards, 1991) and Martin's model (Martin and Ruiz, 2001).

The adoption of these models was made on the basis of the following theoretical assumptions:

a) The panel is assumed to be placed at zero tilt angle.
b) The dust particles are assumed to overlap.
c) The particles are spherical
d) The ratio of the dusty area to the panel area is equal to the ratio of the transmittance with dust to the transmittance without dust.
e) The unshaded area is directly related to the light transmittance to a first approximation.

Though assumption (e) might underestimate the total irradiance that passed through the surface by ignoring the scattered off particles, but the back reflection is expected to counterbalance this effect.

These models are capable of incorporating the various dust sizes and predict the effect of dust obstruction on the output characteristics and other necessary parameters of PV systems irrespective of the location. Simulation was done using MATLAB software.

2.2. Energy Analysis of Dusty Solar PV Panel

In the dusty photovoltaic panel (PV) panel shown in Figure 1, the deposited particles obstruct the incoming solar radiation dwindling the transmissivity. With part of the received incident irradiance converted directly into electricity, a certain percentage is lost to the ambient environment through the dusty glass surface and the back plate.

Figure 1: Dusty photovoltaic panel

If the dusty PV panel operates at steady state condition assumed to be placed at zero tilt angle, the energy balance on the system according to Singh et al. (2018) is given by Equation (1).

$$GA_{pv}\tau_{gD}\left[\alpha_c\beta_c+\alpha_T\left(1-\beta_c\right)\right]=U_{tD}A_{pv}\left(T_{pvD}-T_a\right)+U_bA_{pv}\left(T_{pvD}-T_{bs}\right)+\eta_{cD}\beta_c\tau_{gD}GA_{pv} \quad (1)$$

Where G is incident irradiance (W/m^2), A_{pv} is area of PV panel (m^2), τ_{gD} is dusty glass transmissivity, α_c is PV cell absorptivity, β_c is PV packing factor, α_T is tedlar absorptivity, U_{tD} is dusty PV overall heat lost coefficient (W/m^{2}K), T_{pvD} is dusty PV module temperature(K), T_a is ambient temperature(K), U_b is back module overall heat transfer coefficient (W/m^{2}K), T_{bs} is PV back side temperature (K) and η_{cD} is PV cell efficiency.

The last term of Equation (1) is the amount of energy directly converted into electricity and is dependent on the PV module cell efficiency which is given by Equation (2) (Lamba and Kaushik, 2016).

$$\eta_{cD}=\eta_{ref}[1-\beta_0\left(T_{pvD}-T_{ref}\right)] \quad (2)$$

Where η_{ref} is PV reference efficiency, β_0 is cell temperature coefficient (1/K), T_{ref} is PV reference temperature (K)
The substitution of Equation (2) into Equation (1) and rearrangement gives the dust influenced module temperature expressions in Equation (3).

$$T_{pvD}=\frac{\left(\alpha\tau\right)_{eff}G+U_{tD}T_a+U_bT_{bs}}{U_L} \quad (3)$$

Where:

$$\left(\alpha\tau\right)_{eff}=\tau_{gD}[\alpha_c\beta_c+\alpha_T\left(1-\beta_c\right)-\beta_c\eta_{ref}\left(1+\beta_0T_{ref}\right)] \quad (4)$$

$(\alpha\tau)_{eff}$ is effective transmittance, U_L is overall heat transfer coefficient.
And:

$$U_L=U_{tD}+U_b-\beta_c\beta_0\tau_{gD}\eta_{ref}G \quad (5)$$

The second term on the right hand side of Equation (1) is the energy transferred from the back side of the PV module to the environment and the overall heat transfer coefficient is given by:

$$U_b = \left[\frac{L_{pv}}{k_{pv}} + \frac{L_T}{k_T} \right]^{-1} \tag{6}$$

where L_{pv}, is PV material thickness (m), L_T is tedlar thickness(m), k_{pv} is PV thermal conductivity (W/mK), k_T is tedlar thermal conductivity (W/mK).

The first term of Equation (1) is the energy transferred through the dusty glass through conduction, convection and radiation. The overall heat transfer coefficient with the dust influence is given as:

$$U_{tD} = \left[\frac{L_g}{k_g} + \frac{1}{h_0} + \frac{L_D}{k_D} \right]^{-1} \tag{7}$$

Where L_g is glass thickness (m), L_D is effective thickness of uniformly distributed particles(m), k_g and k_D are glass and dust thermal conductivities respectively (W/mK), h_0 is heat loss transfer coefficient (W/m^{2}K).

The combined convective and radiative heat transfer coefficient is given as:

$$h_0 = 5.7 + 3.8v \tag{8}$$

The effective thickness of the dust deposit can be obtained by assuming that the particles are uniformly distributed over the PV panel surface. Therefore, it is analogous to a total volume equal to $A_{pv}L_D$ and a single volume of particles (incorporating total dust mass, product of particles and average density of particle is $M_D / N\rho$ (Katzan and Edwards, 1991; Wang et al., 2017). Since the above-named cubical volume will be equal to the entire dust volumes, it is given as M_D / ρ. Therefore, the effective thickness of the dust particle is given as:

$$L_D = \frac{M_D}{A_{pv}\rho} \tag{9}$$

Where M_D is mass of dust(kg), ρ is particle density (kg/m^3).

Another essential parameter that is majorly affected by dust deposition through which the module temperature, efficiency and output characteristics (such as voltage and current) are altered from their normal operational values is the glass transmissivity. The module temperature is related to the back plate temperature and temperature differential change as given by Equation (10) noting that the differential change in temperature from the panel to the tedlar is very small.

$$T_{pvD} = T_{bs} + \delta T \tag{10}$$

The tedlar serves as the critical backsheet component, providing long-term durability for photovoltaic modules in all weather conditions. Lee and Taya (2012) carried out a thermal study of PV panel under varying conditions and observed that the difference in the module and tedlar temperature are between 0.6 ^{o}C and 0.8 ^{o}C. Boulfaf and Chaoufi (2017) carried out a study on the properties of a photovoltaic system. They discovered that the temperature difference between the glass, down to the tedlar layers is not more than 1 ^{o}C. Based on literature, this study adopted a module and tedlar temperature difference of 0.65 ^{o}C.

2.3. Overlay Transmission Models

This model was developed by NASA to describe the influence of dust deposition on solar PV modules (Katzan and Edwards 1991) as reported in Wang et al., 2017). The overlay transmission model is feasible under the following theoretical assumptions: (a) All the dust particles are spherical. (b) The ratio of the dusty

area to the panel area is equal to the ratio of the transmittance with dust to the transmittance without dust. Given that the cross-sectional area of a dust particle is ϖ, the probability that it will shadow a given point is ϖ / A_{pv}. Then, the probability of the region is not covered by dust particle is $\left(1-\varpi / A_{pv}\right)$. For *N* particles with relative transmittance γ, the probability of a point still remaining unshaded and may overlay is given as $\left(1-\gamma\varpi / A_{pv}\right)^{N}$. Note that the cumulative effect (i.e., without overlapping) $\left(1-N\gamma\varpi / A_{pv}\right)$ is unrealistic at extreme values of *N*.

Considering and introducing the effect of particles with different sizes, and numbering them from *1,2, 3... n,* the probability of a non-obstructed point is given as:

$$\left(1-\gamma\varpi_1 / A_{pv}\right)^{N_1}\left(1-\gamma\varpi_2 / A_{pv}\right)^{N_2}\left(1-\gamma\varpi_3 / A_{pv}\right)^{N_3}...\left(1-\gamma\varpi_n / A_{pv}\right)^{N_n} \tag{11}$$

Introducing a dummy parameter defined as $j_n = A_{pv} / \gamma\varpi_n$. The number of a set of particles *N*, assuming spherical for this case is given as:

$$N_n = \frac{M_{D_n}}{\rho V} = \frac{3M_{D_n}}{\rho 4\pi R_n^{\,3}} = \frac{3M_{D_n} j_n \gamma}{4\rho A_{pv} R_n} \tag{12}$$

From the assumption that is spherical:

$$\frac{\tau_{gD}}{\tau_g} = \frac{F}{F_0} = \left[\left(1-\frac{1}{j_1}\right)^{j_1}\right]^{\frac{3M_{D_1}\gamma}{4\rho A_{pv}R_1}}\left[\left(1-\frac{1}{j_2}\right)^{j_2}\right]^{\frac{3M_{D_2}\gamma}{4\rho A_{pv}R_2}}\left[\left(1-\frac{1}{j_3}\right)^{j_3}\right]^{\frac{3M_{D_3}\gamma}{4\rho A_{pv}R_3}}...\left[\left(1-\frac{1}{j_n}\right)^{j_n}\right]^{\frac{3M_{D_n}\gamma}{4\rho A_{pv}R_n}} \tag{13}$$

Where *F* is area of an unobscured surface (m^2), F_0 is original area of obscured surface (m^2), $\tau_{g\theta D}$ dusty glass transmissivity influenced by incident angle and τ_g is glass transmissivity.

From Equation (13) as $A_{pv} / \varpi_n \to \infty$, $\left(1-\frac{1}{j_n}\right)^{j_n} \to \exp(-1)$ hence, Equation (13) can be rewritten as:

$$\frac{\tau_{gD}}{\tau_g} = \exp\left[-\frac{3\gamma}{4\rho A_{pv}}\left(\frac{M_{D_1}}{R_1}+\frac{M_{D_2}}{R_2}+\frac{M_{D_3}}{R_3}+...+\frac{M_{D_n}}{R_n}\right)\right] \tag{14}$$

If the particles are assumed to be of the same size for simplification purpose, the above equation becomes:

$$\frac{\tau_{gD}}{\tau_g} = \exp\left(-\frac{3M_D\gamma}{4\rho A_{pv}R}\right) \tag{15}$$

This model was further modified including the effect of the incident angle of incoming radiation by assuming that each particle cast an oval shadow on the surface with minor and major axis being *R* and X_a+X_b respectively as shown in Figure 2.

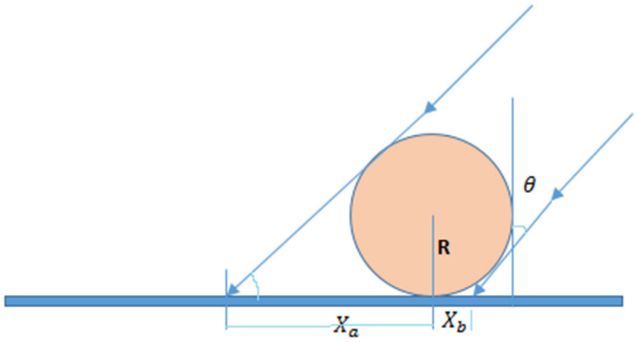

Figure 2: Incident angle schematics of a dust particle

From Figure 3, the shadow area is given by (Zang et al., 2011) as:

$$F_s = \pi R \frac{X_a + X_b}{2} = \frac{\pi R^2}{\cos\theta} = \frac{\varpi}{\cos\theta} \tag{16}$$

Where F_s is dust shadow area (m^2), R is dust radius or minor axis (m), $X_a + X_b$ is the major axis (m), ϖ is dust cross sectional area (m^2) and θ is angle of incidence (^{o}).

This effect was further combined with Equation (15) and the expression with the transmissivity ratio being dependent on the incident angle can be rewritten as:

$$\frac{\tau_{g\theta D}}{\tau_g} = \exp\left(-\frac{3M_D\gamma}{4\rho A_{pv} R\cos\theta}\right) \tag{17}$$

From Equation (17), the effective transmittance and total transfer coefficient can be obtained by substituting Equation (17) into Equation (4) and Equation (5) and replacing the transmittance with the incident angle modified transmittance yields:

$$(\alpha\tau)_{eff,N} = \tau_g \exp\left(-\frac{3M_D\gamma}{4\rho A_{pv} R\cos\theta}\right)[\alpha_c\beta_c + \alpha_T(1-\beta_c) - \beta_c\eta_{ref}(1+\beta_0 T_{ref})] \tag{18}$$

$$U_{L,N} = U_{tD} + U_b - \beta_c\beta_0\eta_{ref} G\tau_g \exp\left(-\frac{3M_D\gamma}{4\rho A_{pv} R\cos\theta}\right) \tag{19}$$

2.4. Martin Model

This model was derived based on the relative module angular loss and the ASHRAE incident angle modifier. Unlike the overlay transmission model developed by NASA that depends directly on the deposited mass and particle sizes, this model depends on the pollution level and incident angle. The expression for incident angle modification by ASHRAE (American Society of Heating, Refrigerating and Air-Conditioning Engineers) without dust influence is given as (ASHRAE, 1985):

$$\frac{\tau_{g\theta}}{\tau_g} = 1 - b_0\left(\frac{1}{\cos\theta} - 1\right) \tag{20}$$

where the adjustable parameter, b_o varies for different PV module and when unknown, a general value of 0.07 is used. $\tau_{g\theta}$ is glass transmissivity influenced by incident angle without dust and τ_g is glass transmissivity. The ASHRAE modifier had shown conspicuous disadvantages at angles greater than 80° and does not incorporate the effect of dust (clean model). However, the Martin model was modified incorporating the influence of dust and given as (Martin and Ruiz 2001; Luque and Hegedus 2003):

$$\frac{\tau_{g\theta D}}{\tau_g}=\left(\frac{\tau_{g\theta D}}{\tau_g}\right)_{\theta=0}\left[1-\frac{\exp\left(-\frac{\cos\theta}{\mu}\right)-\exp\left(-\frac{1}{\mu}\right)}{1-\exp\left(-\frac{1}{\mu}\right)}\right] \tag{21}$$

Where μ is the pollution level given averagely as 0.21 and associated with degree of dirtiness which is characterized by $\left(\frac{\tau_{g\theta D}}{\tau_g}\right)_{\theta=0}$ (Luque and Hegedus, 2003). Similarly, from Equation (21) the expression for the effective transmittance and total transfer coefficients are given by Equations (22) and (23) respectively:

$$(\alpha\tau)_{eff,M}=\tau_g\left(\frac{\tau_{g\theta D}}{\tau_g}\right)_{\theta=0}\left[1-\frac{\exp\left(-\frac{\cos\theta}{\mu}\right)-\exp\left(-\frac{1}{\mu}\right)}{1-\exp\left(-\frac{1}{\mu}\right)}\right][\alpha_c\beta_c+\alpha_T(1-\beta_c)-\beta_c\eta_{ref}(1+\beta_0 T_{ref})] \tag{22}$$

$$U_L=U_{tD}+U_b-\beta_c\beta_0\eta_{ref}G\tau_g\left(\frac{\tau_{g\theta D}}{\tau_g}\right)_{\theta=0}\left[1-\frac{\exp\left(-\frac{\cos\theta}{\mu}\right)-\exp\left(-\frac{1}{\mu}\right)}{1-\exp\left(-\frac{1}{\mu}\right)}\right] \tag{23}$$

From all equations obtained for the dust influence, Equation (3) can now be modified, altering the module temperature as influenced by dust and other parameters such as efficiency, current, and voltage.

2.5. Output Characteristics and Losses of the PV Module with Soiling

For a dusty PV panel, it has been identified that the amount of dust influences the temperature of the module. This in turn changes other parameters such as photo currents, diodes reverse saturation current that depends on temperature. The electrical circuit of a dusty PV module is shown in Figure 3.

Applying the Kirchhoff's current law to the PV system (Lamba and Kaushik, 2016):

$$I_{pvD}=n_p I_{phD}-n_p I_0\left[\exp\left\{\frac{q\left(V_{pvD}+I_{pvD}R_s\right)}{k_B T_{pvD} n_{id} n_s}\right\}-1\right]-\frac{V_{pvD}+I_{pvD}R_s}{R_{sh}} \tag{24}$$

Where I_{pvD} is dusty PV current (A), η is PV system efficiency, q is heat loss(W), V_{pvD} is dusty PV voltage (V), R_s is series resistance (ohms), R_{sh} is shunt resistance (ohms), n_{id} is diode identity factor, n_s is number of PV cells in series, $I_{0,}$ is diode reverse saturation current (A).

The shunt resistance of the cell is much higher than the load resistance. Hence, the equation can be rewritten as:

$$I_{pvD} = n_p I_{phD} - n_p I_0 \left[\exp\left\{ \frac{q\left(V_{pvD} + I_{pvD} R_s\right)}{k_B T_{pvD} n_{id} n_s} \right\} - 1 \right] \tag{25}$$

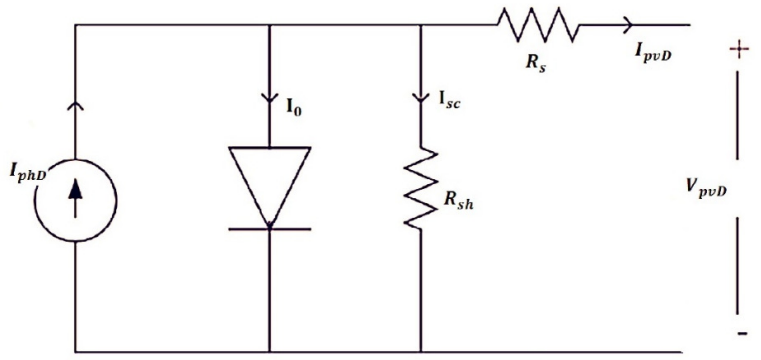

Figure 3: Equivalent electrical circuit for a PV

The dust influenced photo and diode reverse saturation currents are given respectively as (Lamba and Kaushik, 2016):

$$I_{phD} = \left[I_{sc,ref} + k_i \left(T_{pvD} - T_{ref} \right) \right] \frac{G}{G_{ref}} \tag{26}$$

$$I_0 = I_{0,ref} \left(\frac{T_{pvD}}{T_{ref}} \right)^3 \exp\left[\frac{qE_g}{k_B n_{id}} \left(\frac{1}{T_{ref}} - \frac{1}{T_{pvD}} \right) \right] \tag{27}$$

where $I_{sc,ref}$ is short circuit current (A), k_i is current temperature coefficient(mA/K), E_g is band gap energy (eV)

The power produced from the PV system is given by Equation (28).

$$P_{pvD} = I_{pvD} V_{pv} = V_{pv} \left(n_p I_{ph} - n_p I_0 \left[\exp\left\{ \frac{q\left(V_{pv} + I_{pvD} R_s\right)}{k_B T_{pv} n_{id} n_s} \right\} - 1 \right] \right) \tag{28}$$

The efficiency in terms of the module parameters can be calculated from Equation (28) as:

$$\eta_D = \frac{V_{pvD}}{\beta_c \tau_g G A_{pv}} \left(n_p I_{ph} - n_p I_0 \left[\exp\left\{ \frac{q\left(V_{pvD} + I_{pvD} R_s\right)}{k_B T_{pvD} n_{id} n_s} \right\} - 1 \right] \right) \tag{29}$$

The fraction of power loss resulting from dust deposition can be obtained from Equation (30).

$$\xi = \frac{P_{pv} - P_{pvD}}{P_{pv}} = 1 - \left(\frac{P_{pvD}}{P_{pv}} \right) \tag{30}$$

Where ξ is PV power loss fraction, P_{PV} is PV output power (W), P_{PvD} is dusty PV output power(W).

Similarly, the fraction of efficiency and transmissivity losses are given by Equations (31) and (32) as:

$$\eta_{loss} = \frac{\eta - \eta_D}{\eta} = 1 - \frac{\eta_D}{\eta} \tag{31}$$

Where η_{loss} is PV efficiency loss fraction, η_D is dusty PV cell efficiency and η is PV system efficiency.

$$\tau_{loss} = 1 - \left(\frac{\tau_{gD\theta}}{\tau_g} \right) \tag{32}$$

Where τ_{loss} is glass transmissivity loss fraction, $\tau_{g\theta D}$ dusty glass transmissivity influenced by incident angle and τ_g is glass transmissivity.

2.6. Computational Algorithm

All the formulated equations resulting from the analysis were solved using the high-performance computational software, MATLAB, a high-level computer language built around the idea of an interactive programming environment. It contains large numbers of functions that utilize proven numerical libraries. The entire simulation process is directed by programme as shown in the flowchart of Figure 4.

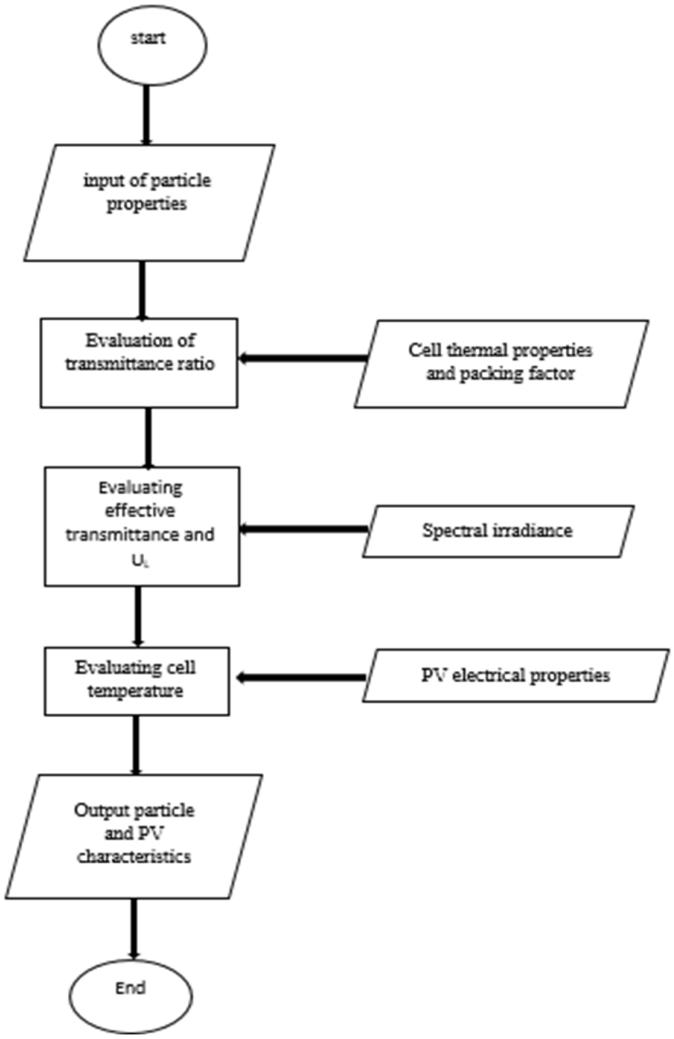

Figure 4: Flow chart for output and PV characteristics

The overlay model takes into account the dusty solar panel referred to as modified model because it includes the effect of incident angle of incoming radiation. It also accounts for dust free solar panel referred to as

clean model in the simulation for purpose of comparison, while the Martin model remained unchanged. The expected results via the established models were compared with existing experimental results. The study was carried out with data from Siemens SP75 PV module (Najafi and Woodbury, 2013) and the module parameters are shown in Table 1.

Table 1: Siemens SP75 PV module parameters (Najafi and Woodbury, 2013)

PV parameters	Values
$I_{sc,ref}$	9.6 A
$I_{0,ref}$	0.118 μA
R_s	0.0018 ohms
T_{ref}	300 K
k_i	2.06 m A/^{o}C
k_v	-0.077 V/^{o}C
β_0	0.003 K^{-1}
Dimensions	1200 mm×527 mm×34 mm
η_{ref}	12%
n_{id}	1.5
n_s	36
L_{pv}	0.0003 m
K_{pv}	0.036 W/mK
L_g	0.003 m
K_g	1 W/mK
β_c	0.85
τ_g	0.95
α_c	0.88
α_T	0.5
L_T	0.0005 m
K_T	0.033 W/mK
E_g	1.12 eV
V	2 m/s

3. RESULTS AND DISCUSSION

The plots showing the three models (modified, clean and Martin models) for different parameters are shown in Figures 5,7,10, 13. It is observed that the three models have been established for both dusty and dust free PV surfaces. The models are capable of incorporating the various dust sizes and predicting the effect of dust obstruction on the output characteristics and other necessary parameters of PV systems irrespective of the location. Simulation was done using MATLAB software. However, the overlay transmission model which was developed by NASA took into account the dusty solar panel referred to as modified model because it includes the effect of incident angle of incoming radiation. It also accounts for dust free solar panel referred to as clean model in the simulation for purpose of comparison, while the Martin model remained unchanged.

For the measurements carried out, a deposited mass of 5 g on a surface area of 0.632 m^2 (material density of 7.91 gm^{-2}), particle density of 2000 kg/m^3 (Wang et al., 2017), size range from 0.2 μm to 40 μm, and thermal conductive resistance to dust particle is believed to be 1.2% of the thermal conductive resistance of glass.

The plot of transmissivity against the incident angles for the three models is shown in Figure 5. The Martin and modified transmission models' graphical curves show a decrease in transmission in the glass through the deposited dust particles as compared to the clean model (no dust model). The decrease of incident angle from 0^0 to 60^0 showed very small deviation and steepened sharply beyond 60^0 with both dust models (modified and Martin models) agreeing with negligible variations in their respective curves. Figure 6 shows

the plot of transmissivity loss against mass density for different incident angles for dusty models (modified and Martin). The graph showed conformity of the results to real situation in that the transmission loss increases simultaneously with increasing deposited dust mass density and increasing incident angle. As a result, the reflectivity of the surface will increase with increasing mass of deposited particles resulting to higher loss of heat to the surrounding as compared to a dust free surface (Mohammad et al., 2016; Wang et al., 2017). Figure 7 is the plot of PV power output against irradiance for the three models at zero incident angle. It shows that the power output for a dusty PV panel (under the Martin and modified model) is less than the power output for a dust free panel (clean model) since the PV cells of the dusty panel will receive less radiation in comparison to the dust free module which results from obstruction and high reflectivity as established in Figures 5 and 6. This implies that dust limits the performance of PV panels. Figure 8 is the plot of power output variation against mass density at different incident angles for G=1000W/m^2. The figure showed that there is power output reduction as mass density increases with increase in different incident angles for G=1000W/m^2. The power reduction was observed to be most at incident angle of 50^0 and less with incident angle of 0^o.

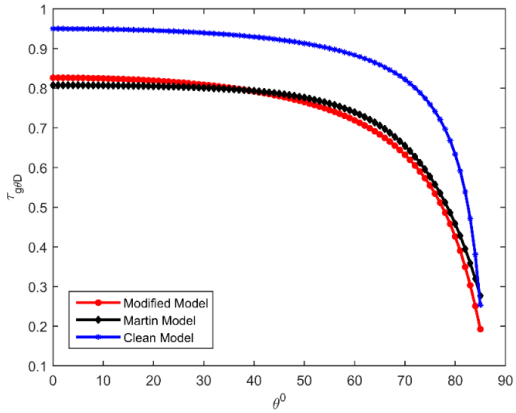

Figure 5: Transmissivity variation with incident angles for the three models

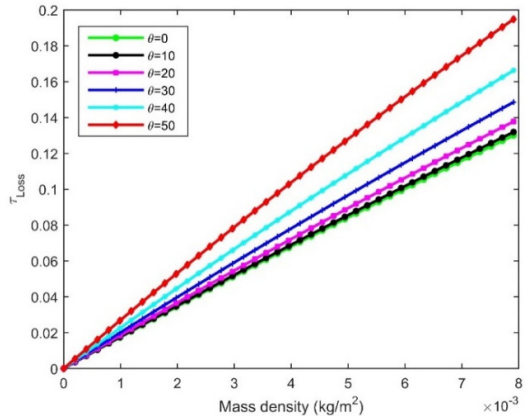

Figure 6: Transmissivity loss fraction variation with deposited dust mass density at different incident angles

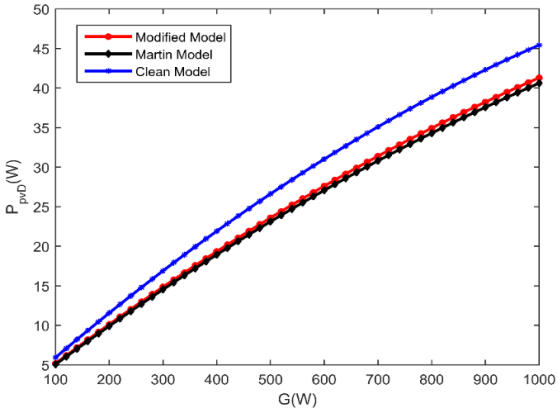

Figure 7: PV power output variation against irradiance for the three models at zero incident angle

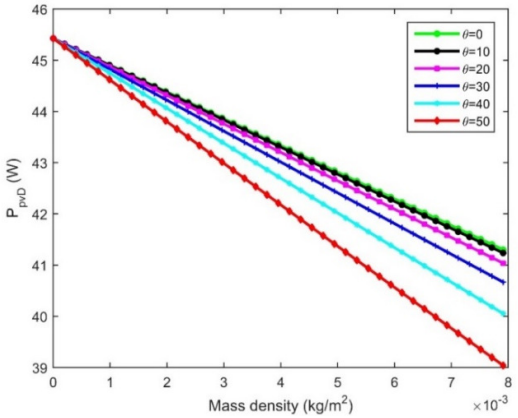

Figure 8: PV power variation with deposited dust mass density at different incident angles for G=1000 W/m^2

The plot in Figure 9 is PV power loss against mass density. It showed that the PV power loss fraction increases as incident angle increases for the simulated condition at about 20.9 %. In addition, as the incident angle increases the intermediate dispersion from the previous value increases simultaneously with highest value corresponding to the highest mass deposit. The plot of PV module efficiency at varying irradiance at zero incident angle for the three models is shown in Figure 10. It can be observed that from the graph that increases in varying irradiance at zero incident angle decreases the PV module efficiency for all the models with Martin and modified models dropping sharply compared to the clean model. As expected from the discussions on the PV power and transmission graphs, the Martin and modified models (dust obstruction models) have efficiency values less than the clean model with the dispersion decreasing as the incident irradiance increases resulting from impairing the transmission of the radiation received by the PV cells by dust particles.

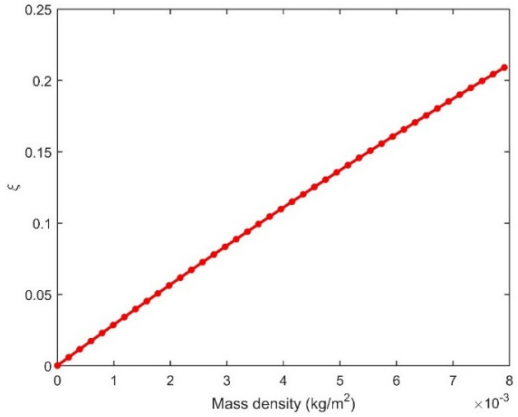

Figure 9: PV power loss fraction variation with deposited dust mass density for G=1000 W/m^2

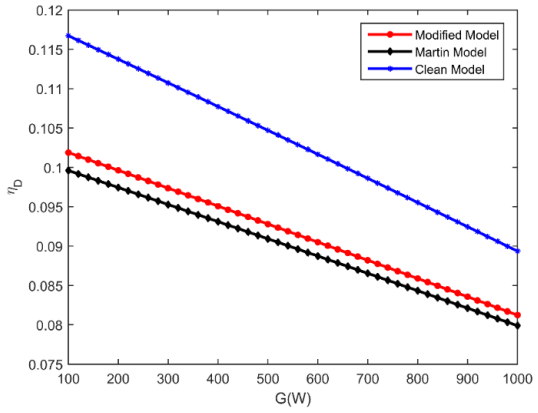

Figure 10: PV efficiency for the three Models at varying incident Irradiance at zero incident angle

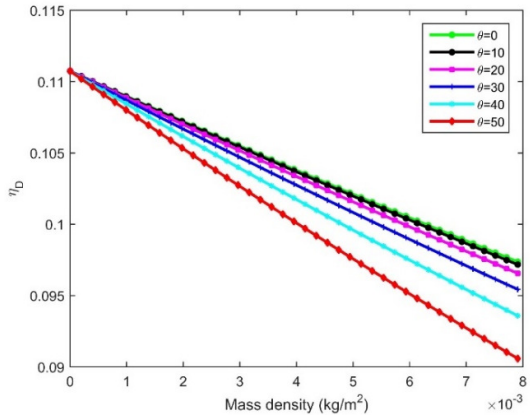

Figure 11: PV efficiency variation with deposited dust mass density at different incident angles for a solar irradiance (G=1000W/m^2)

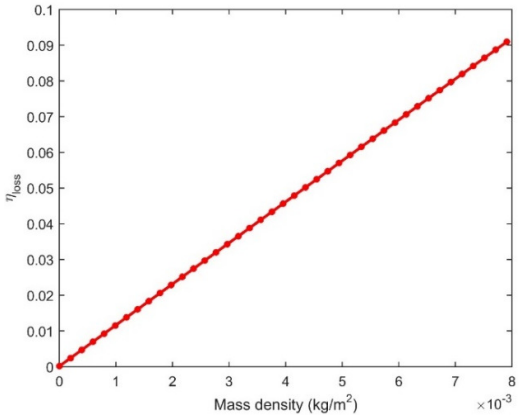

Figure 12: PV efficiency loss fraction variation with deposited dust mass density for G=1000W/m^2

Figure 11 expatiated that the increasing deposited mass quantity automatically reduces the efficiency of the PV module under the operational assumed conditions in this study, the efficiency curve shows a maximum efficiency of about 12.1%. Figure 12 is the PV efficiency loss fraction variation with deposited dust mass density for solar irradiance of G=1000 W/m$^{2.}$. It showed that the PV efficiency loss fraction increases as

the dust mass density increases (Mohammad et al., 2016). As the quantity and area covered by the dust particle continued to spread on the solar panel, the efficiency of the PV system reduces.
Figure 13 shows the result of the plot of current – voltage (I-V) characteristic of the three different models. From the graph, the clean model seemed to have higher values for both the current and voltage of the PV system compared to the Martin and modified model. The nature of the graph was as a result of the particle obstruction effect on the photocurrent and diode saturation current due to the transmission losses in the incident radiation and in turn its effect on the PV module temperature. The plots in Figures 14 and 15 are the graphical comparison of the modified model with experimental results carried out (Abhishek et al., 2017) in Karnataka, India.

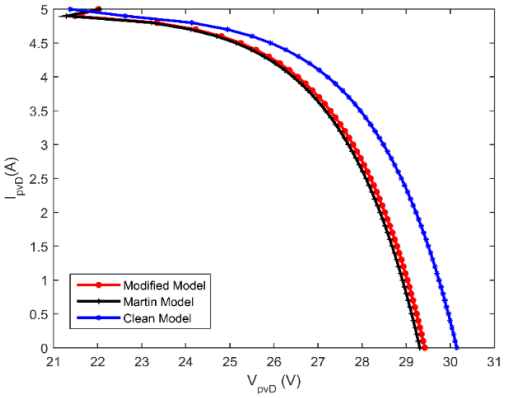

Figure 13: Current-voltage (I-V) characteristics for the three models

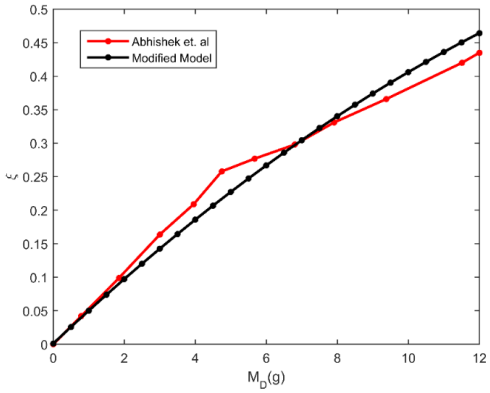

Figure 14: Experimental comparison of the PV power loss fraction

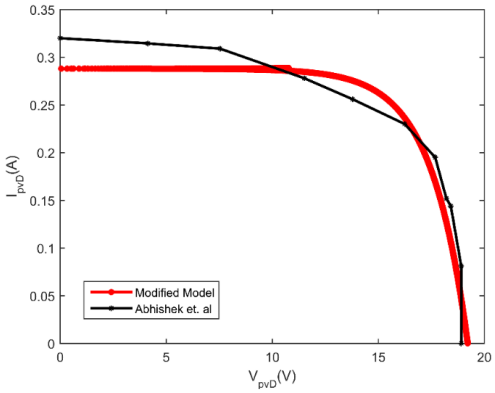

Figure 15: Experimental comparison of the current-voltage (I-V) characteristics

The experiment was carried out using a twenty watts polycrystalline PV module at 545 W/m^2 constant solar radiation. The reason for the comparison is that the validation of experimental result was done at approximately the same environmental condition with the modified model. It adopted a sieve analysis process and the dust was distributed uniformly on module surface with the help of strainer. Figure 13 was the graphical comparison of the power loss fraction with varying mass of dust deposition up to 12 g on a surface area of 0.213 m^2. From the graph, the results showed a certain percentage of fits and deviations up to 6.3% of the power loss. It also showed that the power loss increases as the mass of particles increases. Figure 15 showed the current-voltage (I-V) characteristics of the module with 5 g (23.47 g/m^2 mass density) of dust particles deposited on the surface. From the open circuit voltage to about 10 volts, the graph had a very bad fit, and beyond 10 volts, it had a good fit. It was observed to deviate with a percentage difference of about 9%.

From the basic assumptions made in the modelling and the obtained graphical results, the deviations from the practical values can be based on the following factors:

i. Environmental relative humidity possibly resulting to condensation of water on the panel surface.
ii. Hydrated level of dust particles.
iii. Wind speed interrelationship with the particles and adhesive forces.
iv. Dispersed placement of dust particles even under the overlay condition. This factor might result to underestimating the total radiation that actually passed through the glass as a result of the dispersed particles because several inter-particle heat transfer, particle and glass reflection etc. will take place simultaneously, though the back reflection may reduce the effect.

4. CONCLUSION

In this study, the theoretical obstruction analysis of overlaid deposited dust particles on a PV surface was carried out with the aid of developed transmission models, energy balance relation and electrical analysis of PV systems for different dust sizes and mass of given sets regardless of the location. The overlay obstruction models were simulated, and the simulation results showed that the transmissivity of a dusty PV surface is less than that of a dust free surface and reduces more as the deposited mass increases. As the mass increases, more heat is lost to the environment as the increasing particles increases the reflectivity (decreases transmissivity). Also, incident angle has very little effect on the transmissivity. At incident angles 60^0 and beyond, it showed severe effect. The adverse effects of the particles on the PV do not only depend on the mass of dust deposited but also on the type of dust. However, the deposited mass drastically showed adverse effect simultaneously on the PV output power and efficiency. From the study, percentage reduction of about 20.9% and 9.1% was observed for a mass density of 7.91 kgm^{-2} for both the power output and efficiency respectively, and the reduction shows a proportional increase with the dust mass. In addition, as the particles impair the irradiance transmission, the photo current and diode reverse saturation current are altered resulting to decrease in the PV current and voltage simultaneously. In comparison with experimental results carried out in Karnataka, India the maximum percentage deviation from the experimental result is 6.3% and 9% for the power loss and current-voltage(I-V) characteristics of the system, respectively.

5. CONFLICT OF INTEREST

There is no conflict of interest associated with this work.

REFERENCES

Abdullah, M.M., Mohammed, H.G., Hmood, J. and Al-bassam, S.S. (2014). Analysis of adhesion of dust particles on glass surfaces. *International Journal of Applied or Innovation in Engineering and Management,* 3, pp. 109-112

Abhishek, T.K., Murthy, C and Aruna, M. (2017). Experimental investigation of dust effect on PV module performance. *Global Journal of Research in Engineering,* 17, pp. 35-39.

Ahmed, Z., Kazem, H.A. and Sopian, K. (2013). Impact of Some Environmental Variables with Dust on Solar Photovoltaic (PV) Performance: Review and Research Status. *International Journal of Energy and Environment,* 7, pp. 152-159.

Al-Waeli, A.H.A., Sopian, K., Kazem, H.A. and Chaichan, M.T. (2017). PV/T (photovoltaic/thermal): Status and future prospects. *Renewable and Sustainable Energy Review,* 77, pp. 109-130.

American Society of Heating, Refrigerating and Air-Conditioning Engineers (ASHRAE), (1985). *Methods of Testing to determine the Thermal Performance of Solar Collectors*. New York: American Society of Heating, Refrigeration, and Air Conditioning Engineers.

Appels, R., Lefevre, B., Herteleer, B., Goverde, H., Beerten, A., Paesen, R. and Poortmans, J. (2013). Effect of soiling on Photovoltaic Modules. *Solar Energy,* 96, pp. 283-291.

Bouchalkha, A. (2008). Modeling of dust effect on solar panels. *The Second International Energy 2030 Conference Abu Dhabi*, UAE, pp. 234-238.

Boulfaf, N. and Chaoufi, J. (2017). Identification of thermal parameters of a solar photovoltaic panelin three dimensional using finite element approach. *International. Journal of Renewable Energy Resources.* 7, pp. 578-588

Dadas, S.N., Patil, P.S., Shinde, N.N and Wagh, M. M. (2016). Evaluation of effect of dust on polycrystalline silicon solar cell. *International. Research Journal of Engineering and Technology,* 3, pp. 2781-2785.

Hashim, E.T. (2013). Effect of dust and shadow on the efficiency of photovoltaic solar module at Baghdad climate conditions. *The Iraqi Journal. for Mechanical and Material Engineering,* 13, 769-783.

Hashim, E.T and Hussien, T.A. (2016). Dust effect on the efficiency of silicon monocrystalline solar modules at different tilt angles at al-jadryia climate conditions. *Journal of Engineering*. 22, pp. 56-73.

Kaldellis, J.K., Fragos, P. and Kapsali, M. (2011). Systematic experimental study of the pollution deposition impact on the energy yield of photovoltaic installations. *Renewable Energy,* 36, pp. 2717-2724.

Katzan, C.M. and Edwards, J.L. (1991). Lunar dust transport and potential interactions with power system components. NASA Contractor Report 4404.

Lamba, R. and Kaushik, S.C. (2016). Modeling and performance analysis of a concentrated photovoltaic–thermoelectric hybrid power generation system. *Energy Conversion Management,* 115, pp. 288-298.

Lee, Yand Taya, A.A.O. (2012). Finite element thermal analysis of a solar photovoltaic module. *Energy Procedia,* 15, pp. 413-420.

Luque, A and Hegedus, S. (2003). *Handbook of Photovoltaic Science and Engineering*. John Wiley & Sons.

Martin, N and Ruiz, J. (2001). Calculation of the pv modules angular losses under field conditions by means of an analytical model. *Solar Energy Material and Solar Cells,* 70, pp. 25-38.

Mekhilefa, S., Saidur, R. and Kamalisarvestani, M. (2012). Effect of dust, humidity and air velocity on efficiency of photovoltaic cells. *Renewable and Sustainable Energy Review*s, 16, pp. 2920-2925.

Menoufi, K. (2017). Dust accumulation on the surface of photovoltaic panels: introducing the photovoltaic soiling index (PVSI). *Sustainability,* 9, pp. 1-12.

Mohammad, R.M., Hashim, H., Chandima, G., Mohd, A.R., Mohammed, I.R., and Shahrooz, H. (2016). Power loss due to soiling on solar panel: A review. *Renewable and Sustainable Energy Reviews,* 59, pp. 1307 -1316.

Najafi, H and Woodbury, K.A. (2013). Modeling and analysis of a combined photovoltaic thermoelectric power generation system. *Journal of Solar Energy Engineering* 135, pp. 1-8.

Paudyal, B.R., Shakya, S.R., Paudyal, D.P and Mulmi, D.D. (2017). Soiling-induced transmittance losses in solar PV modules installed in Kathmandu Valley. *Renewawables*, 4, pp. 1-8.

Samadhiya, A and Pandey, R. (2016). Analysis of pv panels under various weather conditions. *International Journal of Emerging Research in Management and Technology,* 5, pp. 53-61.

Sarver, T., Al-Qaraghuli, A. and Kazmerski, L.L. (2013). A comprehensive review of the impact of dust on the use of solar energy: History, investigations, results, literature, and mitigation approaches. *Renewable and Sustainable Energy Reviews*, 22, pp. 698-733.

Sayyah, A., Horenstein, M.N. and Mazumder, M.K. (2014). Energy yield loss caused by dust deposition on photovoltaic panels. *Solar Energy,* 107, pp. 576–604.

Singh, S., Ibeagwu, O.I. and Lamba, R (2018). Thermodynamic evaluation of irreversibility and optimum performance of a concentrated PV-TEG cogenerated hybrid system. *Solar Energy,* 170, pp. 896–905.

Syed, S.A., Husam and W.M. (2014). Fundamental studies on dust fouling effects on PV module performance. *Solar Energy,* 107, pp. 328-337.

Wang, J., Gong, H. and Zou, Z. (2017). Modeling of dust deposition affecting transmittance of PV modules. *Journal of Clean Energy Technology,* 5, pp. 217-221.

Zang, J.B., Wang, Y.W. and Wang, X.D. (2011). Computation model and experiment of dust deposition affecting transmittance of photovoltaic module. *Acta Energiae Solaris Sinica,* 35, pp. 624-629.

Zorrilla-Casanova, J., Piliougine, M., Carretero, J., Bernaola, P., Carpena, P., Mora-López, L. and Sidrach-de-Cardona, M. (2011). Analysis of dust losses in photovoltaic modules. *World Renewable Energy Congress,* 8, pp. 2985-2992.